

## OPEN

# Emodin Alleviates Intestinal Barrier Dysfunction by Inhibiting Apoptosis and Regulating the Immune Response in Severe Acute Pancreatitis

Qi Zhou, MD,\*† Hong Xiang, MD,\* Han Liu, MD,‡ Bing Qi, MD,§ Xueying Shi, MS,\*† Wenhui Guo, MS,\* Jiacheng Zou, BS,|| Xueting Wan, BS,\* Wenjing Wu, BS,\* Zhengpeng Wang, MS,\* Wenhui Liu, MS,\* Shilin Xia, MD,\* and Dong Shang, MD\*†§

**Objective:** The intestinal barrier injury caused by severe acute pancreatitis (SAP) can induce enterogenous infection, further aggravating the inflammatory reactions and immune responses. This study aimed to test the hypothesis that emodin protects the intestinal function and is involved in the immune response in SAP.

**Methods:** The network pharmacology was established using the Swiss target prediction and pathway enrichment analysis. The SAP mice model was induced by cerulein (50 µg/kg) and lipopolysaccharide (10 mg/kg) hyperstimulation. The pharmacological effect of emodin in treating SAP was evaluated at mRNA and protein levels by various methods.

**Results:** The network analysis provided the connectivity between the targets of emodin and the intestinal barrier-associated proteins and predicted the BAX/Bcl-2/caspase 3 signaling pathway. Emodin alleviated the pathological damages to the pancreas and intestine and reduced the high concentrations of serum amylase and cytokines in vivo. Emodin increased the expression of intestinal barrier-related proteins and reversed the changes in the apoptosis-related proteins in the intestine. Simultaneously, emodin

regulated the ratio of T helper type 1 (T<sub>H</sub>1), T<sub>H</sub>2, T<sub>H</sub>17, γδ T cells, and interferon γ/interleukin 17 producing γδ T cells.

**Conclusions:** These findings partly verified the mechanism underlying the regulation of the intestinal barrier and immune response by emodin.

**Key Words:** emodin, severe acute pancreatitis, intestinal dysfunction, apoptosis, inflammatory immune response

**Abbreviations:** AP - acute pancreatitis, ELISA - enzyme-linked immunosorbent assay, HE - hematoxylin and eosin, IL-1β - interleukin 1β, MLN - mesenteric lymph node cells, SAP - severe acute pancreatitis, SIRS - systemic inflammatory response syndrome, TNF-α - tumor necrosis factor α, ZO-1 - Zonula occludens 1

(*Pancreas* 2021;50: 1202–1211)

Acute pancreatitis (AP) is one of the most common gastrointestinal disorders with increasing incidence leading to high hospital admissions worldwide.<sup>1</sup> According to the updated Atlanta classification, 12% of patients develop severe acute pancreatitis (SAP), despite the mild self-limited property of AP. Patients experiencing SAP have a mortality rate of 20% to 30% due to its rapidly evolving complications, posing a significant clinical challenge and financial burden to society.<sup>2,3</sup> Recently accumulated pieces of evidence has shown that gastrointestinal failure is a crucial organ failure and an independent predictor of the poor outcome in AP, mainly mediated by the injury to the intestinal barrier.<sup>4–6</sup> The intestine acts as a functional barrier and the largest immune organ; hence, impairing the intestinal barrier could exaggerate the severity of SAP by increasing the intestinal permeability, microbial infections, bacterial translocation, and release of proinflammatory substances.<sup>7,8</sup> Therefore, the intestine drives the local inflammation in SAP leading to distant organ dysfunction. The management of the SAP-related intestinal barrier injury is an effective strategy to alleviate the aggravation of SAP.

The Chinese herb, rhubarb, is a principal component of Chinese herbal formulas (eg, Yinchenhao, Dachengqi decoctions) and has been extensively applied in the clinical treatment of acute abdominal diseases, such as AP.<sup>9,10</sup> To elucidate their therapeutic roles in the treatment of SAP, the ingredients of the herbs have been extensively assessed via in silico, in vitro, and in vivo experiments. Emodin, as a predominant compound of rhubarb, has been reported to inhibit vacuole formation in the acinar cells,<sup>11</sup> attenuate autophagy response,<sup>12</sup> and protect against the oxidative stress and inflammasome signals in SAP.<sup>13,14</sup> However, the role of emodin in the intestinal barrier injury and immune response caused by SAP is still limited.

In the present study, a network pharmacology-based strategy was designed to identify the connectivity between the targets of emodin and the intestinal barrier-associated proteins. The pathological changes in the pancreas and intestine were observed. We continued to detect the inflammatory factors in the serum of the

From the \*Clinical Laboratory of Integrative Medicine, The First Affiliated Hospital of Dalian Medical University; †Institute (College) of Integrative Medicine, and ‡Department of Oral Pathology, Dalian Medical University; §Department of General Surgery, The First Affiliated Hospital of Dalian Medical University, Dalian, China; and ||Department of Molecular, Cellular, & Developmental Biology, University of California, Santa Barbara, Goleta, CA.

Received for publication August 20, 2020; accepted August 17, 2021.

Address correspondence to: Shilin Xia, MD, Clinical Laboratory of Integrative Medicine, The First Affiliated Hospital of Dalian Medical University, No. 222 Zhongshan Rd, Dalian 116023, China (e-mail: shilin320@126.com); or Dong Shang, MD, Department of General Surgery, Pancreatic-Biliary Center, The First Affiliated Hospital of Dalian Medical University, No. 222 Zhongshan Road, Dalian 116023, China (e-mail: shangdong@dmu.edu.cn).

The authors declare no conflict of interest.

This research was supported by the National Key Research and Development Program of China (No. 2018YFE0195200), the National Natural Science Foundation of China (No. 81703871 and No. 81873156), Natural Science Foundation of Liaoning Province (2020-MS-265), Scientific Research of Department of Education in Liaoning Province (LZ2019045), and Doctoral Start-up Foundation of Liaoning Province (No. 20170520408).

Q.Z., H.X., and H.L. contributed equally as first authors.

S.X. and D.S. conceived and designed the experiments. Q.Z. and H.X. performed flow cytometry assay and drafted the manuscript. H.L. and B.Q. carried out animal experiments. X.S., X.W., and W.W. conducted the integrated bioinformatics analysis. W.G. and J.Z. performed hematoxylin and eosin staining and enzyme-linked immunosorbent assay. Z.W. and W.L. performed western blot analyses. All authors have read and approved the final manuscript.

Supplemental digital contents are available for this article. Direct URL citations appear in the printed text and are provided in the HTML and PDF versions of this article on the journal's Web site ([www.pancreasjournal.com](http://www.pancreasjournal.com)).

Copyright © 2021 The Author(s). Published by Wolters Kluwer Health, Inc. This is an open-access article distributed under the terms of the Creative Commons Attribution-Non Commercial-No Derivatives License 4.0 (CCBY-NC-ND), where it is permissible to download and share the work provided it is properly cited. The work cannot be changed in any way or used commercially without permission from the journal.

DOI: 10.1097/MPA.0000000000001894

animal model. Furthermore, the levels of the intestinal barrier-related proteins were examined. Subsequently, the proportion of the immune cells, including T helper type 1 (T<sub>H</sub>1) cells, T<sub>H</sub>2 cells, T<sub>H</sub>17 cells, Treg cells, and  $\gamma\delta$  T cells were evaluated. We aimed to illustrate that the use of emodin may alleviate the severity of intestinal injury and is involved in immune regulation during the progression of SAP.

## MATERIALS AND METHODS

### Analysis of Compound Targets and Construction of Protein-Protein Interactions

First, a canonical SMILES code of emodin was obtained from PubChem (<https://pubchem.ncbi.nlm.nih.gov>), which collects and stores the chemical information on compounds and substances. The SMILES result was CC1=CC2=C(C(=C1)O)C(=O)C3=C(C2=O)C=C(C=C3)O, which was computed by OEChem 2.1.5 (<https://www.eyesopen.com/oechem-tk>; OpenEye, Santa Fe, NM). Next, we submitted the result of SMILES to SwissTargetPrediction (<http://www.swisstargetprediction.ch>; Swiss Institute of Bioinformatics, Lausanne, Switzerland).<sup>15</sup> We used this web tool to estimate the most probable molecular targets of emodin. An interaction network between the targets and the intestinal barrier-related proteins was constructed using the STITCH database (Version 5.0, <http://stitch.embl.de>; STITCH Consortium, Dresden, Germany). Finally, this network connectivity was analyzed and visualized using Cytoscape software (Version 3.7.2, Cytoscape Consortium, San Diego, Calif). The Cytoscape bioinformatics software enabling the visualization of protein-protein interactions (PPIs), and a cluster screening of complicated molecular networks was used.<sup>16</sup>

### Materials and Reagents

Emodin and sodium carboxymethyl cellulose (CMC-Na) were purchased from Solarbio Science and Technology Co (Beijing, China). Cerulein and the 4 kDa fluorescent dextran-FITC (DX-4000-FITC) were purchased from Sigma-Aldrich Co (St Louis, Mo). The mouse AMY ELISA kits were purchased from Lengtong Biotech (Shanghai, China). The mouse tumor necrosis factor  $\alpha$  (TNF- $\alpha$ ) and interleukin 1 $\beta$  (IL-1 $\beta$ ) ELISA kits were purchased from Fine Biotech Co (Wuhan, China). The antioccludin (Cat. Ab216327), antizoonula occludens 1 (ZO-1, Cat. Ab96587), and antioccludin 4 (Cat. Ab15104) were purchased from Abcam (Cambridge, United Kingdom). The anti-BAX (Cat. YT0455) and anti-Bcl-2 (Cat. YM3041), anti-caspase 3 (Cat. YM3435), and anti- $\beta$ -actin antibodies (Cat. YM3435) were purchased from the Immunoway Biotechnology Company (Plano, Tex). The red blood cell lysate was purchased from Tianjin Haoyang Biological Manufacturer (Tianjin, China). The Leukocyte Activation Cocktail (with BD GolgiPlug), Fixation and Permeabilization Kit (BD Golgistop protein transport inhibitor), Fixable Viability Stain 780, PE Hamster Antimouse  $\gamma\delta$  T-Cell Receptor, Alexa Fluor 647 Rat, Antimouse IL-17A, Percp-cy 5.5 Hamster, Antimouse CD3e, FITC Rat Antimouse CD4, Alex-Fluor700 Rat Antimouse IFN- $\gamma$ , PE-Cy7 Rat Antimouse IL-4, and Mouse BD Fc Block were obtained from BD Biosciences (Franklin Lakes, NJ). The kits for detection the amylase and creatinine, aspartate aminotransferase, alanine aminotransferase, and urea nitrogen were purchased from Nanjing Jiancheng Bioengineering Institute (Nanjing, China). Terminal deoxynucleotidyl transferase dUTP nick-end labeling (TUNEL) assay kit was obtained from KeyGEN BioTECH (Jiangsu, China).

### Animal Experiments

Male C57BL/6 J mice (7–8 weeks old) with a bodyweight of 20 g (standard deviation [SD], 2 g) were obtained from the

Experimental Animal Center of the Dalian Medical University. The mice were housed under a stress-free and specific pathogen-free condition, with a constant room temperature of 22°C (SD, 3) and 70% (SD, 5%) relative humidity and maintained under a 12-hour light/12-hour dark cycle. All the animals were provided with standard laboratory chow and water ad libitum before the experiment and acclimatized for 1 week before the experiment. Before inducing SAP, the mice were subjected to fasting for 12 hours but had access to water. The medical ethics committee of the Dalian Medical University approved all the animal experimental protocols (AEE18072), which complied with the recommendations of the National and International Guidelines for the Care and Use of Laboratory Animals.

### Model Establishment and Groups

The animals were divided randomly into 3 groups ( $n = 5$ , where “n” refers to the number of animals in each group). The mice in the control group were injected with normal saline (50  $\mu$ g/kg). The SAP and emodin-treated groups were induced by the intraperitoneal injection of cerulein (50  $\mu$ g/kg) 7 times, and LPS (10 mg/kg) was incorporated into the final injection of cerulein. In the 48-hour treatment group, the animals were pretreated with emodin (dissolved in 0.5% CMC-Na) at a dose of 70 mg/kg before the first intraperitoneal injection of cerulein, and emodin was administered at an interval of 8 hours between the two. Both the control and SAP groups were administered an equivalent volume of 0.5% CMC-Na solution. The animals were killed 48 hours after the last injection of LPS by injecting pentobarbital (100 mg/kg body weight) intraperitoneally. The blood samples were collected from the heart for biochemical parameter analysis of the serum. The pancreas and part of the distal ileum were promptly fixed in a 10% neutral buffered formaldehyde solution for further histological examination. The segments of the distal ileum were isolated, washed with cold phosphate-buffered saline, snap-frozen in liquid nitrogen, and stored at  $-80^{\circ}\text{C}$  for further experiments. In addition, the spleen was freshly isolated for the immune cell analysis.

### Hematoxylin and Eosin Staining

Samples of the pancreas and terminal ileum were fixed with 10% neutral buffered formaldehyde solution and embedded in paraffin wax. The deparaffinized and rehydrated serial sections (5  $\mu$ m) were stained with hematoxylin and eosin (HE). The slides were visualized under a microscope for morphologic changes like pancreatic edema, acinar cell necrosis, adipose necrosis, hemorrhage, and inflammation, and scored in a blinded manner according to the previous description.<sup>17,18</sup> The histological damage of the ileum was evaluated with scores between 0 and 5 as described previously.<sup>19</sup>

### Immunohistochemistry and TUNEL Staining

Paraffin-embedded sections were subsequently processed. For immunohistochemistry, antibody dilutions were as follows: claudin 4 (1:100), ZO-1 (1:200), and occludin (1:10). The staining intensity and extent (positively stained area) were evaluated independently by 2 pathologists independently. Besides, sections were stained with TUNEL to evaluate in situ cell apoptosis. In brief, the slides were incubated with 50  $\mu$ L of TUNEL reaction mixture in a humid atmosphere for 1 hour at 37°C and then incubated for 0.5 hours with an antibody specific for fluorescein-conjugated horseradish peroxidase (HRP).

### Intestinal Permeability In Vivo

To detect the intestinal permeability, 4000 Da fluorescent dextran-FITC (500 mg/kg body weight, 125 mg/mL) was

gavaged to the mice 3 hours before the experiment. The serum was collected and diluted in an equal volume of PBS. The fluorometric analysis was performed using a fluorescence spectrophotometer (PerkinElmer, Wellesley, Mass) at an excitation wavelength of 485 nm and emission wavelength of 535 nm as previously described.<sup>20</sup> A standard curve was obtained by diluting FITC-dextran in the nontreated plasma diluted with PBS (1:3 vol/vol). All the procedures were performed strictly protected from light.

### Enzyme-Linked Immunosorbent Assay: Measurement of Amylase Activity and Inflammatory Cytokines

The blood samples were collected from the heart and centrifuged at 3000g for 20 minutes at 4°C, and the serum was stored frozen at -80°C. The serum levels of amylase, TNF- $\alpha$ , and IL-1 $\beta$  were measured using a commercial kit according to the manufacturer's instructions.

### Cell Isolation From the Spleen

To prepare the lymphocytes, the spleen was removed from the mice, minced into small pieces, and ground gently with a syringe core on a stainless-steel mesh under aseptic conditions. The red blood cell lysates were used to remove the red blood cells. The lymphocytes were passed through a 100- $\mu$ m nylon mesh to remove the tissue debris.

### Flow Cytometry Analysis

To analyze the changes in the immune cells during SAP, the lymphocytes were immediately harvested from the spleen and detected as follows: for an obvious and better cytokine production assay, the total lymphocytes were incubated with a leukocyte activation cocktail containing phorbol ester, PMA, ionomycin, and brefeldin A in the RPMI 1640 complete medium at 37°C for 6 hours. Before staining, the cell suspension was preincubated with Fc block at 4°C for 15 minutes. The Fixable Viability Stain 780 (FVS780) was used to exclude the dead cells. Surface staining was performed using the CD3, CD4, and  $\gamma\delta$  TCR antibodies. For intracellular staining, the cells were fixed and permeabilized using a fixation and permeabilization kit for 50 minutes at 4°C and finally stained with the antibodies against IL-4, IL-17A, and IFN- $\gamma$ . The flow cytometry analysis was performed using a flow cytometer (Fortessa; BD Biosciences), and the data were analyzed using Flowjo software (Version 10.6.0; BD Life Sciences, Ashland, Ore).

### Western Blotting Analysis

Protein from the distal ileum was extracted using a protein extraction kit (Invent SD001/SN002; Plymouth, Minn). The protein concentrations were determined using the BCA assay kit. Equal amounts of protein samples were subjected to SDS-PAGE in a mini gel apparatus (Mini-PROTEAN II; Bio-Rad, Hercules, Calif) and then transferred onto the nitrocellulose membranes. The membranes were blocked with 5% fat-free milk for 2 hours and were incubated with antibodies against occludin (1:1000), ZO-1 (1:500), claudin 4 (1:100), BAX (1:500), Bcl-2 (1:500), caspase 3 (1:500), and  $\beta$ -actin (1:1000) overnight at 4°C. Subsequently, the membranes were washed with Tris-buffered saline with Tween-20 (TBST) and incubated with the HRP-conjugated secondary antibodies for 1 hour at room temperature. The protein bands were visualized with a Western Bright ECL Western blotting HRP Substrate kit and analyzed using the Image Lab software (Bio-Rad).

### Statistical Analysis

The data represent the mean of at least 3 independent experiments and are presented as the mean  $\pm$  standard error of the mean (SEM). The GraphPad Prism 7.0 software (GraphPad, San Diego, Calif) was used for the statistical analysis. The statistical analysis of the quantitative multigroup was compared using the 1-way analysis of variance and Tukey test. Differences were considered statistically significant at  $P < 0.05$  or  $P < 0.01$ .

## RESULTS

### Emodin's Targets Are Involved in the Regulation of Intestinal Barrier-Related Proteins and the Apoptosis Pathway

To explore the network of emodin's potential targets and provide clues to connect emodin and the intestinal barrier, we obtained the SMILES data for emodin based on PubChem, to identify 43 potential targets of emodin with higher scores in the SwissTargetPrediction database. Next, an interaction network was constructed between the network of emodin's target and intestinal barrier-related proteins, as well as the apoptosis pathway. Figure 1 shows that the network of emodin targets was associated with OCLN and ZO-1 (known as the tight junction protein), as well as BAX, Bcl-2, and caspase 3. Then, the analysis of this network was expanded from 15 to 45 proteins based on the PPI enrichment. We found that the expanding network was involved in

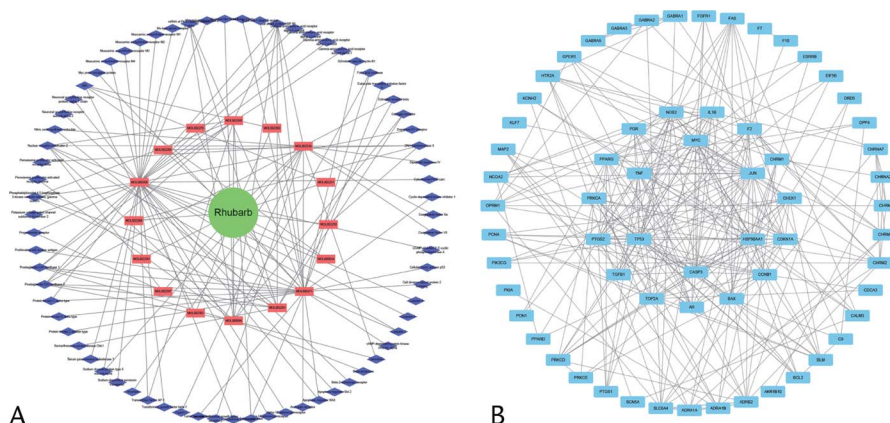


**FIGURE 1.** Network pharmacology. A, Herb compound-targets network of rhubarb (red rectangle represents compounds and the blue diamond represents targets). B, Compound-related targets in the PPI network (the inside circle represents the hub PPI network).

the biological processes, including apoptosis signaling pathway (false discovery rate:  $3.20\text{e-}28$ ), cellular response to stress (false discovery rate:  $3.82\text{e-}23$ ), and positive regulation of cell communication (false discovery rate:  $2.13\text{e-}16$ ). Our analysis highlighted that emodin may regulate the intestinal barrier by targeting intestinal barrier-related proteins and apoptosis-related proteins.

### Emodin Ameliorated the Severity and the Inflammatory State of SAP in Mice

The results of serum biochemical parameters and HE staining showed that emodin at the dose of 70 mg/kg did not exhibit toxicology for major organs (Supplemental Fig. 1, <http://links.lww.com/MPA/A899>). The level of amylase in the serum from the SAP group was significantly higher than in the control group, and it was markedly decreased after the emodin treatment

(Fig. 2A). Subsequently, the concentrations of the proinflammatory cytokines, TNF- $\alpha$ , and IL-1 $\beta$  were evaluated in the serum. As shown in Figures 2B and C, the markedly increased level of amylase in the SAP group was decreased compared with that in the emodin group. These results suggested that emodin exerts potent protective effects against inflammation in SAP mice.

### Emodin Reversed Pathological Phenotype of Pancreatic Injury in the SAP Mice

To assess the pathological changes among the different groups, we performed HE staining. As shown in Figure 2D, the pancreatic pathology in the control group had normal morphology. In contrast, marked disruption characterized by extensive enlarged interlobular interspaces, acinar necrosis, hemorrhage, and inflammatory infiltration was observed in the SAP mice.

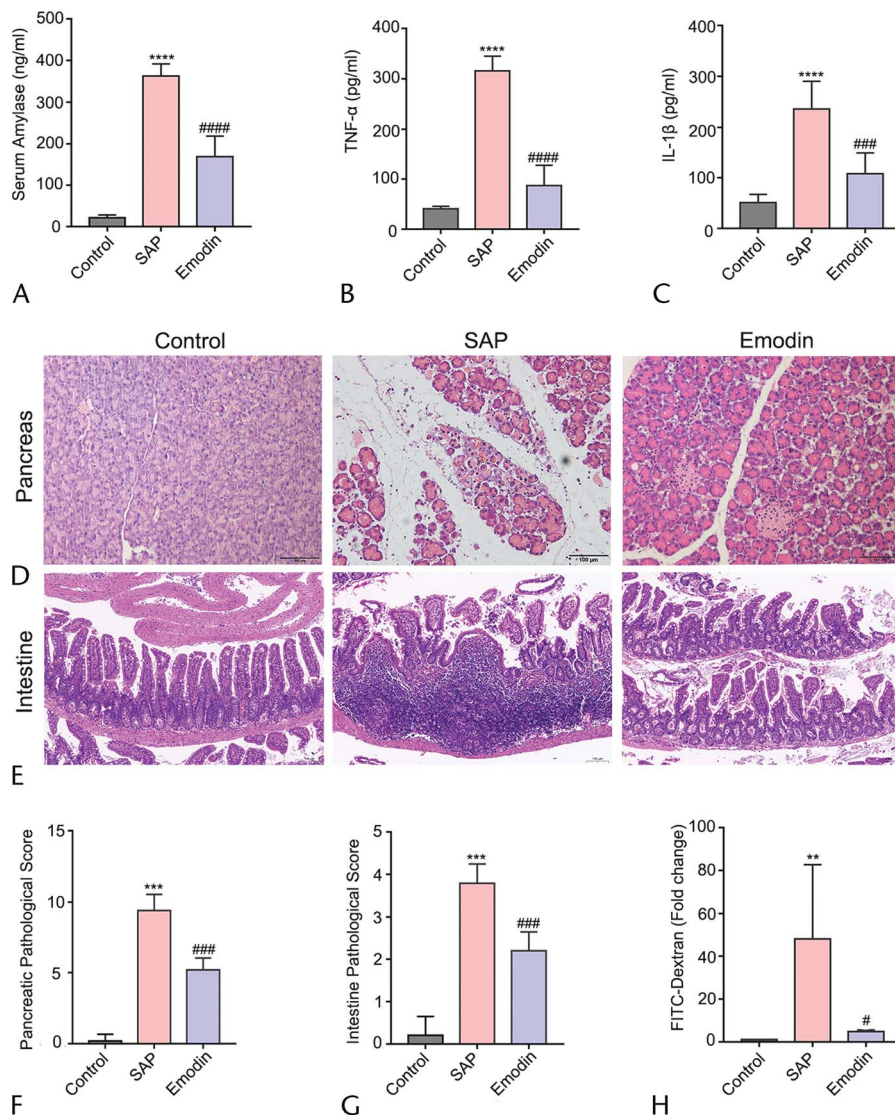


**FIGURE 2.** Effects of emodin on pancreatitis based on amylase, proinflammation cytokines, and histological morphology. A–C, Serum concentrations of amylase, TNF- $\alpha$ , and IL-1 $\beta$  of all 3 groups. D–E, The HE staining (original magnification  $\times 200$  and  $\times 400$ ). F–G, The pathological score of the pancreas and intestine after SAP induction and emodin treatment. H, The evaluation of intestinal permeability. Data are presented as the mean  $\pm$  SEM ( $n = 5$ ), where “ $n$ ” refers to independent values;  $*P < 0.01$ ,  $***P < 0.001$  versus the control group;  $****P < 0.0001$  versus the control group;  $\#P < 0.05$ ,  $###P < 0.001$  versus the SAP group;  $####P < 0.0001$  versus the SAP group.

Moreover, emodin notably decreased the severity of the pancreas histopathology shown by milder damage compared with that in the SAP group. As shown in Figure 2F, high pancreatic pathological scores were evaluated in comparison with that of the control group, but emodin treatment markedly inhibited the pathological changes, which were statistically significantly different from that observed in the SAP group. These results indicated that the model was successfully established by the long-term intraperitoneal injection of cerulein along with a large dose of LPS, and emodin exhibited the potential anti-inflammatory function in SAP.

### Emodin Relieved the Intestinal Barrier Injury in the SAP Mice

Next, HE staining of the intestinal tissue was performed to detect the intestinal changes after the SAP induction. As shown in Figure 2E, the intestinal tissues in the SAP groups consistently exhibited severe damage, including obvious hyperemia and edema and microvilli exfoliation. This phenomenon was attenuated in the emodin-treated group. As shown in Figure 2G, compared with those in the control group, the SAP group demonstrated higher

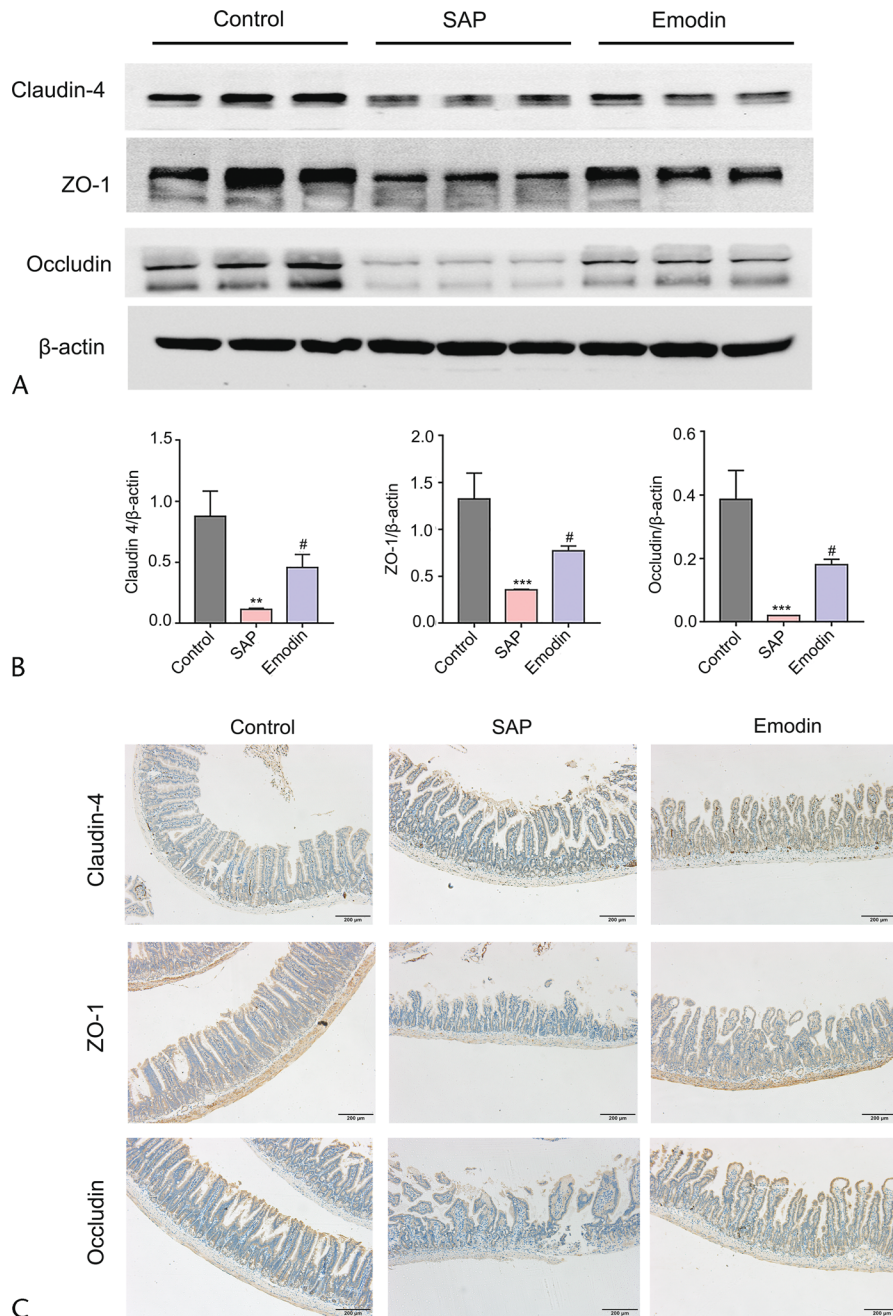


**FIGURE 3.** Changes in the protein level of the intestinal barrier-related mediators, including claudin 4, occludin, and ZO-1 in the different groups. A, Western blot imaging of claudin 4, occludin, and ZO-1. B, The relative expression of claudin 4, occludin, and ZO-1 protein. C, TUNEL staining of intestine sections. \*\* $P < 0.01$  versus the control group; \*\*\* $P < 0.001$  versus the control group; # $P < 0.05$  versus the SAP group.

pathological scores of the intestinal mucosa, but the emodin group showed statistically lower pathological scores than the SAP group. Furthermore, the serum FITC-dextran level is a frequently used indicator for revealing intestinal mucosal mass and integrity. As shown in Figure 2H, it was significantly increased in the mice with SAP, and the effect was reversed after treatment with emodin. This observation suggests that emodin plays a protective role in SAP-related intestinal barrier injury.

### Emodin Upregulated the Mediators to the Intestinal Barrier

In addition to an obvious disruption of the intestinal barrier injury, the expression levels of the intestinal barrier-related proteins, including claudin-4, ZO-1, and occludin, which comprise a tight junction complex for regulating the intestinal permeability, were examined. As shown in Figures 3A and B, all the three proteins were significantly downregulated in the SAP group compared with the control group, whereas the changes in proteins were recovered in the emodin group. The results of immunohistochemistry staining were consistent with results of western blot (Fig. 3C). These results indicate the promising protective effects of emodin against intestinal barrier dysfunction in the SAP mice.

### Emodin Regulated the BAX/Bcl-2/Caspase 3 Pathway in the Intestine of the SAP Mice

To further verify the apoptotic mechanism mediated by emodin predicted previously, we investigated the BAX/Bcl-2/caspase 3 pathway, closely associated with the regulation of both the apoptosis as well as the tight junction complex. As shown in Figures 4A to B, western blotting showed upregulation in the levels of BAX and cleaved caspase 3 (proapoptotic) and downregulation in the expression of Bcl-2 (antiapoptotic) in the SAP group, compared with that in the control group. However, this trend was reversed after the administration of emodin. Thus, the classical BAX/Bcl-2/caspase 3 pathway may participate in intestinal barrier injury, and emodin showed a protective function against intestinal barrier injury, possibly mediated by targeting this pathway. In addition, to evaluate *in situ* cell apoptosis, TUNEL staining was performed, the results of which exhibited that emodin could inhibit apoptosis of intestine in SAP development (Fig. 4C).

### Emodin Regulated the Profile of Immune Cells in SAP Mice

Previous studies have emphasized the importance of T cells in the adaptive immune response.<sup>21–23</sup> Thus, we continued to

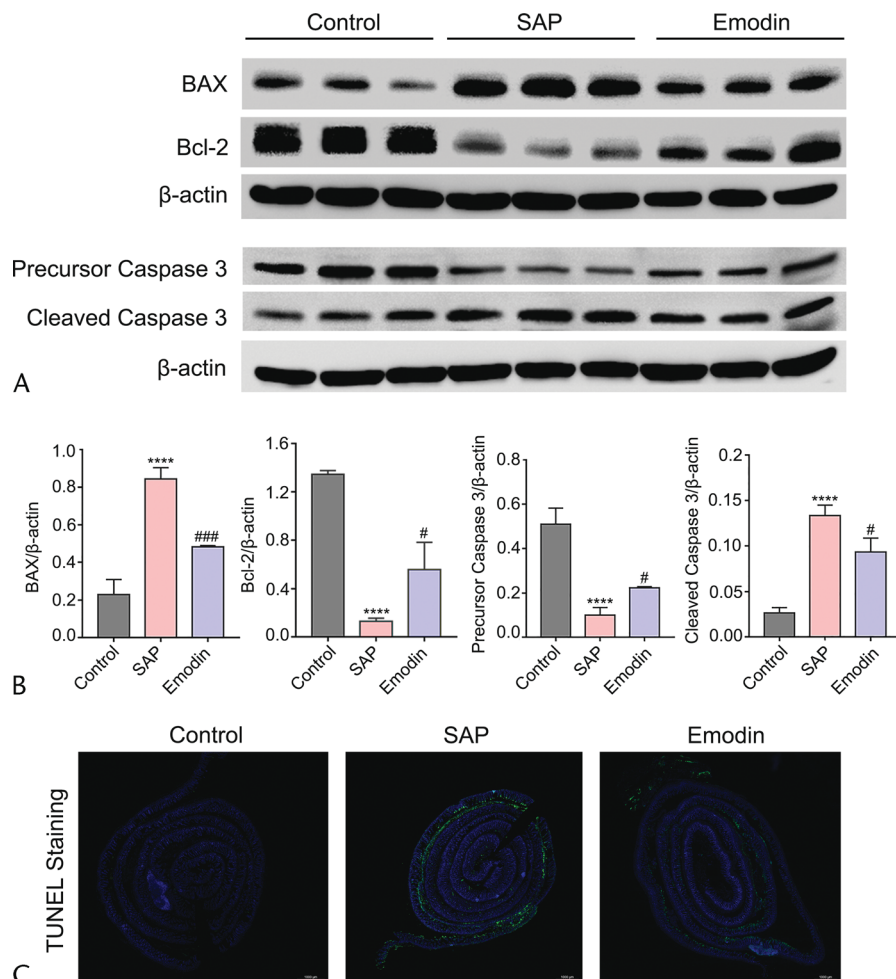


**FIGURE 4.** Changes in the protein levels of the BAX/Bcl-2/caspase 3 signaling pathway in the different groups. A, Western blot imaging of the BAX, Bcl-2, and caspase 3 proteins. B, The relative expression of the BAX, Bcl-2, and caspase 3 protein. C, The expression of claudin 4, ZO-1, and occludin in intestines by immunohistochemistry staining. \*\*\*\* $P < 0.05$  versus the control group; ### $P < 0.001$  versus the SAP group, # $P < 0.05$  versus the SAP group.

explore the activation of the splenic CD4+ T cells by flow cytometry. As shown in Figure 5, increased ratios of TH1 and TH17 cells and a decreased proportion of TH2 cells were detected in the SAP group compared with the control group. Interestingly, emodin reversed the elevated ratio of TH1 and TH17 cells. Subsequently, we detected a significant induction of Tregs in the SAP group compared with that in the control group. However, emodin did not affect the ratio of Tregs. Next, based on the previous studies indicating the emerging role of  $\gamma\delta$  T cells in inflammatory diseases, we measured the activation of the splenic  $\gamma\delta$  T cells. As shown in Figure 6, the number of  $\gamma\delta$  T and IFN- $\gamma$ /IL-17 producing  $\gamma\delta$  T cells was higher in the SAP group than in the control group, while the emodin-induced reversion was significant.

### DISCUSSION

Severe acute pancreatitis, which originates primarily as a sterile local inflammation, has been found to escalate rapidly to the systemic inflammatory response syndrome and organ failure.

It has been recognized that intestinal barrier injury amplifies the severity of SAP. A series of studies have indicated that Chinese medicine plays a pleiotropic role in the progression of inflammatory disorders.<sup>24,25</sup> The therapeutic potential of rhubarb, a Chinese herb, in treatment of abdominal disorders has been well documented. This study illustrated the therapeutic potential of emodin, the principal component of rhubarb, in alleviating the severity of intestinal injury and inhibiting the progression of SAP and aimed to identify the connectivity between the targets of emodin and the intestinal barrier-associated proteins.

First, the molecular targets of emodin were retrieved to construct a connectivity network of these targets in SAP. Furthermore, we determined whether occludin and ZO-1 (also shown as TJP1) were associated with this network of emodin targets. Emodin was also found to regulate the BAX/Bcl-2/caspase 3 pathway to inhibit cell apoptosis. Collectively, the results of our study suggested that emodin influences the intestinal barrier simultaneously mediating the tight junctions and apoptosis. Given that the compensatory anti-inflammatory response syndrome not only initiated a mainly

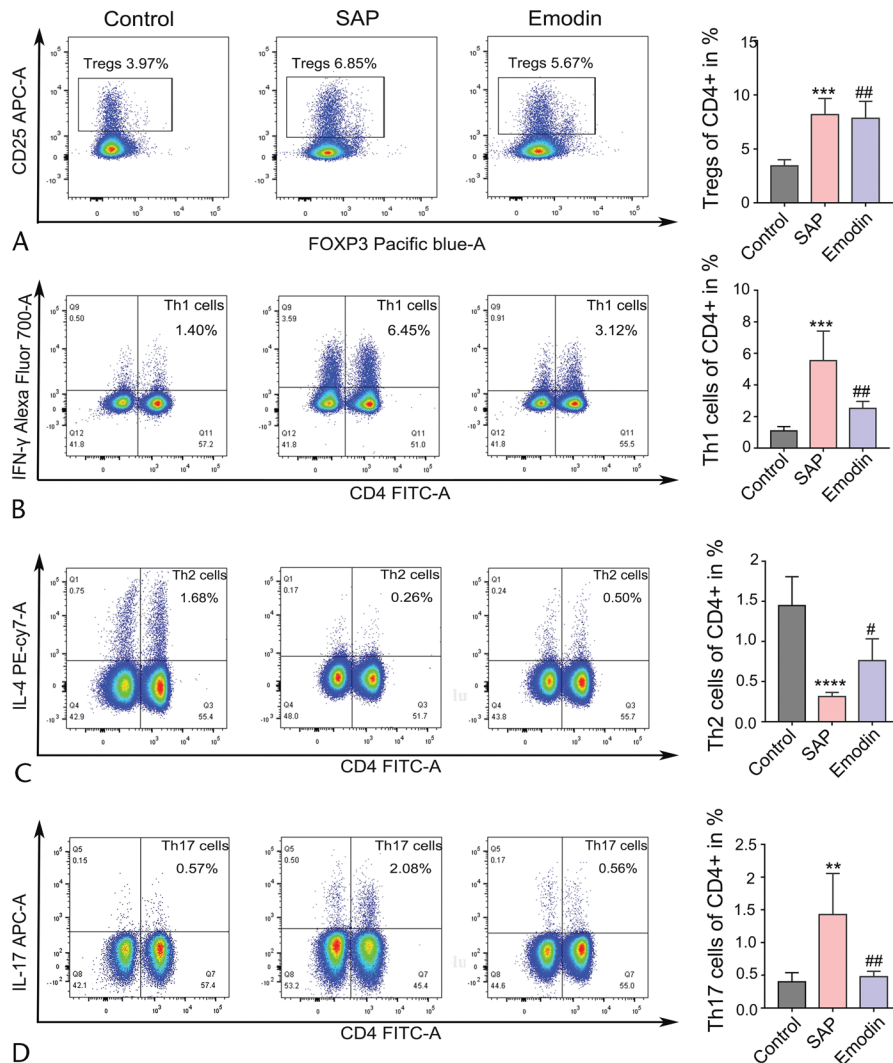


**FIGURE 5.** Effects of emodin on the subsets of CD4+ T cells in the spleen of the SAP mice. The ratio of the TH1 cells (A), TH2 cells (B), TH17 cells (C), and Treg cells (D) in the CD4+ T cells of the spleen, analyzed by flow cytometry in mice. \*\**P* < 0.01 versus the control group; \*\*\**P* < 0.001 versus the control group; \*\*\*\**P* < 0.0001 versus the control group; #*P* < 0.05 versus the SAP group; ##*P* < 0.01 versus the SAP group; NS, not significant.

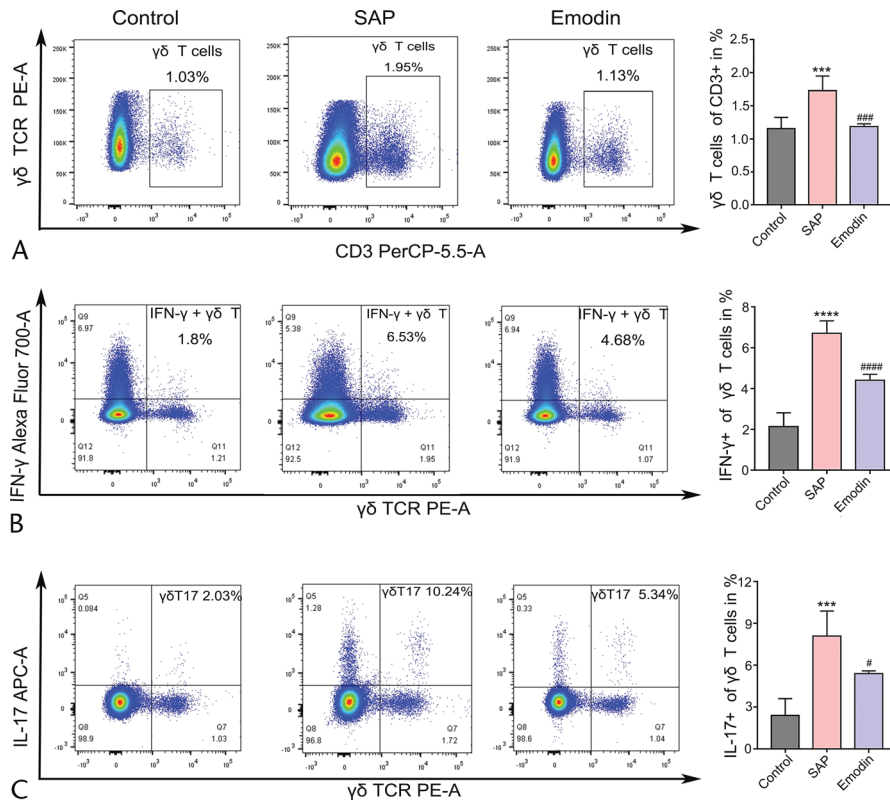


**FIGURE 6.** Effects of emodin on the changed subsets profile of the  $\gamma\delta$  T cells in the spleen of the SAP mice. The ratio of the  $\gamma\delta$  T cells in the CD3+ T cells (A), the ratio of IFN- $\gamma$  (B), IL-4 (C), and IL-17 (D) producing  $\gamma\delta$  T cells in the total  $\gamma\delta$  T cells of spleen, analyzed by flow cytometry in mice. \*\*\* $P < 0.001$  versus the control group; \*\*\*\* $P < 0.0001$  versus the control group; # $P < 0.05$  versus the SAP group; ### $P < 0.001$  versus the SAP group; #### $P < 0.001$  versus the SAP group.

anti-inflammatory role but also induced immunosuppression, the change in the immune cells after emodin treatment was assessed. In summary, the current data substantiated the protective function of emodin on the intestinal barrier during SAP by regulating tight junctions, apoptosis, and immune responses.

Our current study has demonstrated that emodin treatment decreases the pathological score and permeability of the intestine. The components of the tight junction complex were found to increase after the emodin treatment. The intestinal barrier injury presumably accounts for the accelerated severity of SAP. The tight junction complex of the intestine is important for maintaining the integrity of the intestinal barrier. The tight junction complex mainly consists of the proteins like claudins, ZO-1, and occludin. This complex constitutes a paracellular structure between the epithelial and endothelial cells to prevent the invasion of toxins, pathogens, and other exogenous substances.<sup>26</sup> The transmembrane proteins like occludin and members of the claudin family form tight junction strands in the extracellular environment. Moreover, the ZO proteins, such as ZO-1, ZO-2, and ZO-3, offer molecular scaffolds by interacting with the claudins and occludin via binding the cytoplasmic tail to the actin cytoskeleton.<sup>27</sup> Lei et al<sup>28</sup> found that emodin decreased the expression of ZO-1 by inhibiting the NF- $\kappa$ B and HIF-1 $\alpha$  signaling pathways in the inflammatory and hypoxic injury of the intestinal epithelial cells. Emodin has also been reported to promote pancreatic claudin-5 and occludin expression and improve the pancreatic paracellular permeability in the AP model of rats.<sup>29</sup> This evidence, thus, indicated that emodin could diminish the intestinal barrier dysfunction caused by SAP. The results of the previous study were in unison with those of

our present study, revealing both the histopathological changes and molecular mechanisms involved in the progression of SAP. Our findings, thus, provide a detailed insight into the molecular mechanism by which emodin mediates protection against the intestinal barrier injury during the progression of SAP.

Apoptosis plays a beneficial role in the acinar damage during AP, which is attributed to the decreased trypsin activity. However, previous studies have verified that the damage of the nonpancreatic organs in AP is primarily induced by apoptosis.<sup>30</sup> Thus, it is necessary to find a strategy to inhibit the mediators of apoptosis in the intestine in SAP. In the current study, we detected an increased expression of BAX and a decrease in the Bcl-2 after SAP induction. Bcl-2 is a crucial antiapoptotic protein that is negatively regulated by BAX. We also found an increase in the cleaved caspase 3 as the final effector to execute the program of apoptosis.<sup>31,32</sup> Moreover, our results verified that emodin treatment reversed these changes. Our results indicate that emodin protects against intestinal barrier injury induced by SAP, possibly via the BAX/Bcl-2/caspase 3 pathway.

In the present study, we observed elevated percentages of Tregs, T<sub>H</sub>1, and T<sub>H</sub>17 cells, but a low percentage of T<sub>H</sub>2 cells in the spleen. Furthermore, emodin inhibited the ratio of the T<sub>H</sub>1 and T<sub>H</sub>17 cells and promoted the ratio of T<sub>H</sub>2 cells. Previous studies have found that the process of pancreatitis is paralleled by the innate and the adaptive immune response.<sup>33</sup> Although the neutrophils and macrophages are responsible for the innate immune system, the T cells assume an essential role in the adaptive immune response.<sup>34</sup> As evident in recent literature, the T cells have vital functions in the immune response. The T helper cells, a subset



of CD4<sup>+</sup> T cells, induce a special immune response. For example, the T<sub>H1</sub> cells produce proinflammatory cytokines, such as TNF- $\alpha$ , IFN- $\gamma$ , and IL-1 $\beta$ , which mediate cellular immunity. In contrast, the T<sub>H2</sub> cells drive anti-inflammatory responses by secreting anti-inflammatory cytokines. Therefore, it may be an effective strategy to reduce the T<sub>H1</sub>/T<sub>H2</sub> ratio, maintain balance, and prevent further deterioration in the patients with SAP. In addition, Tregs also regulate the balance between immune activation and tolerance.<sup>35</sup> Minkov et al<sup>36</sup> have shown that an enhanced ratio of circulating Tregs could be an independent prognostic biomarker in the SAP patients, indicating immune suppression occurring in the early AP. Our findings corresponded to some studies<sup>37</sup> but contradicted the others.<sup>33</sup> The possible reason for this phenomenon is primarily the variability in the immune response observed at multiple time points within different SAP models.

This study has made a novel revelation of the altered profiles of the  $\gamma\delta$  T cells, IFN- $\gamma$ -producing  $\gamma\delta$  T cells, and  $\gamma\delta$  T17 cells in mice with SAP under the influence of cerulein. Recently, the emerging role of  $\gamma\delta$  T cells has attracted more attention because of its potent inflammatory cytokine-producing function under numerous pathophysiological conditions. The  $\gamma\delta$  T cells drive proinflammatory processes by differentiating into IFN- $\gamma$ -producing or IL-17-producing subsets depending on the weak or strong  $\gamma\delta$  TCR signals.<sup>38,39</sup> Interleukin 17 is a proinflammatory cytokine with pleiotropic function and is implicated in imparting protection against bacterial and fungal infection by inducing chemokines, recruiting neutrophils, and activating the T cells and B cells.<sup>40,41</sup> Interleukin 17 plays an essential role in neutrophil chemoattraction, promoting the formation of aggregated neutrophils and hindering the outflow of pancreatic secretion, resulting in focal pancreatitis and determining the severity of pancreatitis.<sup>42</sup> In contrast, the role of IL-17 is controversial for the maintenance of the integrity of the intestinal barrier in inflammatory bowel diseases. Some studies hold beneficial effects, but some support the impaired functions.<sup>43</sup> Recently, IL-17 was reported that it was not only produced by the T<sub>H17</sub> cells but also primarily secreted by the  $\gamma\delta$  T cells in inflammatory disease. Considering the potential of  $\gamma\delta$  T cells, we detected the changes in the  $\gamma\delta$  T cells and their subsets in the spleen. In this study, we found an enhanced proportion of  $\gamma\delta$  T cells, IFN- $\gamma$ -producing  $\gamma\delta$  T cells, and  $\gamma\delta$  T17 cells in the SAP group and a decline in the proportion after emodin administration. The finding of an elevated percentage of  $\gamma\delta$  T and  $\gamma\delta$  T17 is supported by Yan et al.<sup>44</sup> In that study, a transient upregulation of IL-17A expression and  $\gamma\delta$  T influx was found within 3 days in the pancreas of coxsackievirus B3-induced pancreatitis, mediated by promoting neutrophil infiltration and T<sub>H17</sub> induction, suggesting the critical pathogenic effect of  $\gamma\delta$  T17 cells.<sup>44</sup> Our results showed that emodin was involved in the regulation of the immune response in the SAP mice by restoring the balance between the CD4<sup>+</sup> T cells and decreasing the ratio of the  $\gamma\delta$  T cells and their subsets from the spleen. The disrupted adaptive immune system could trigger the translocation of the intestine-derived bacteria, resulting in a systemic inflammatory response and even sepsis in SAP. A previous study has shown rhubarb restores the T<sub>H1</sub>/T<sub>H2</sub> cell balance and decreases the number of Tregs in the small intestinal tissues or mesenteric lymph node cells.<sup>37</sup> Moreover, a novel role of the spleen in SAP was recognized in aggravating the occurrence of the systematic inflammatory responses and multiple organ failure, including intestinal mucosal barrier dysfunction. Thus, we speculated that emodin displayed a protective function by regulating the inflammatory immune response of SAP by maintaining the splenic homeostasis.<sup>45</sup>

Although 5 subsets of T cells were detected, there was a lack of other T cells, such as CD8<sup>+</sup> T cells and T<sub>H9</sub> cells. In the future, the profile of the other T cells needs to be delineated in SAP,

which would enable us to delineate the landscape of the immune response to emodin. In addition, we examined the immune cells from the spleen tissue. The role of the immune cells in the intestines should be confirmed. The T cells were difficult to stabilize in the intestine of SAP mice, because of which, we were unable to record the proportion of the T cell subsets.

Taken together, the present study has demonstrated that emodin protects against intestinal injury via the BAX/Bcl-2/caspase 3 pathway and regulates the immune response in the SAP mice. We herein proposed pieces of evidence that emodin executes a protective function to the intestinal barrier and, concomitantly, influences the immune response in the SAP mice. Therefore, it enhances our understanding of the potential of emodin in SAP.

## CONCLUSIONS

This study was based on the pharmacological network and the network analysis providing the connectivity between the targets of emodin and intestinal barrier-associated proteins, mainly the tight junctions (occludin and claudins) and ZO-1. Furthermore, the pathway enrichment and PPI network analyses showed that emodin plays a vital role in the BAX/Bcl-2/caspase 3 signaling pathway. The data from the in vivo experiments showed that emodin acts as a potential drug for preventing intestinal barrier injury. Emodin was found to promote the intestinal barrier integrity by inhibiting the apoptosis signaling pathway and regulating the immune response simultaneously in the mouse model of SAP. These findings may clinically contribute to the potential therapeutic targets of an important traditional Chinese medicine, rhubarb. Moreover, the underlying targets and pathways of emodin, the main gradient of rhubarb, have been identified partly. Therefore, this study established emodin as a promising therapeutic intervention for treating SAP and intestinal injury.

## ACKNOWLEDGMENTS

The authors thank Ming Li for the help in the spleen cells preparation and Chunlei Liu, Mengwei Li, and Xue Sui for assistance with the flow cytometry assay.

## REFERENCES

- Petrov MS, Yadav D. Global epidemiology and holistic prevention of pancreatitis. *Nat Rev Gastroenterol Hepatol*. 2019;16:175–184.
- Hines OJ, Pandolfi SJ. Management of severe acute pancreatitis. *BMJ*. 2019; 367:l6227.
- Matta B, Gougol A, Gao X, et al. Worldwide variations in demographics, management, and outcomes of acute pancreatitis. *Clin Gastroenterol Hepatol*. 2020;18:1567–1575.e2.
- Agarwala R, Rana SS, Sharma R, et al. Gastrointestinal failure is a predictor of poor outcome in patients with acute pancreatitis. *Dig Dis Sci*. 2020; 65:2419–2426.
- Zhu Y, He C, Li X, et al. Gut microbiota dysbiosis worsens the severity of acute pancreatitis in patients and mice. *J Gastroenterol*. 2019;54:347–358.
- Cui QR, Ling YH, Wen SH, et al. Gut barrier dysfunction induced by aggressive fluid resuscitation in severe acute pancreatitis is alleviated by necroptosis inhibition in rats. *Shock*. 2019;52:e107–e116.
- Scaldeferri F, Pizzoferrato M, Gerardi V, et al. The gut barrier: new acquisitions and therapeutic approaches. *J Clin Gastroenterol*. 2012;46 (suppl):S12–S17.
- Liu J, Huang L, Luo M, et al. Bacterial translocation in acute pancreatitis. *Crit Rev Microbiol*. 2019;45:539–547.
- Su S, Liang T, Zhou X, et al. Qingyi decoction attenuates severe acute pancreatitis in rats via inhibition of inflammation and protection of the intestinal barrier. *J Int Med Res*. 2019;47:2215–2227.

10. Sun W, Chen Y, Li H, et al. Material basis and molecular mechanisms of Dachengqi decoction in the treatment of acute pancreatitis based on network pharmacology. *Biomed Pharmacother.* 2020;121:109656.
11. Li J, Zhou R, Bie BB, et al. Emodin and baicalin inhibit sodium taurocholate-induced vacuole formation in pancreatic acinar cells. *World J Gastroenterol.* 2018;24:35–45.
12. Yu X, Li C, Song H, et al. Emodin attenuates autophagy response to protect the pancreas from acute pancreatitis failure. *Pancreas.* 2018;47:892–897.
13. Zhang Q, Hu F, Guo F, et al. Emodin attenuates adenosine triphosphate-induced pancreatic ductal cell injury in vitro via the inhibition of the P2X7/NLRP3 signaling pathway. *Oncol Rep.* 2019;42:1589–1597.
14. Xia S, Ni Y, Zhou Q, et al. Emodin attenuates severe acute pancreatitis via antioxidant and anti-inflammatory activity. *Inflammation.* 2019;42:2129–2138.
15. Daina A, Michielin O, Zoete V. SwissTargetPrediction: updated data and new features for efficient prediction of protein targets of small molecules. *Nucleic Acids Res.* 2019;47:W357–W364.
16. Su G, Morris JH, Demchak B, et al. Biological network exploration with Cytoscape 3. *Curr Protoc Bioinformatics.* 2014;47:8.13.1–8.13.24.
17. Ma R, Yuan F, Wang S, et al. Calycosin alleviates cerulein-induced acute pancreatitis by inhibiting the inflammatory response and oxidative stress via the P38 MAPK and NF- $\kappa$ B signal pathways in mice. *Biomed Pharmacother.* 2018;105:599–605.
18. Schmidt J, Rattner DW, Lewandrowski K, et al. A better model of acute pancreatitis for evaluating therapy. *Ann Surg.* 1992;215:44–56.
19. Zhang M, Wu YQ, Xie L, et al. Isoliquiritigenin protects against pancreatic injury and intestinal dysfunction after severe acute pancreatitis via Nrf2 signaling. *Front Pharmacol.* 2018;9:936.
20. Tang C, Kamiya T, Liu Y, et al. Inhibition of dectin-1 signaling ameliorates colitis by inducing lactobacillus-mediated regulatory T cell expansion in the intestine. *Cell Host Microbe.* 2015;18:183–197.
21. Gukovskaya AS, Gukovsky I, Algül H, et al. Autophagy, inflammation, and immune dysfunction in the pathogenesis of pancreatitis. *Gastroenterology.* 2017;153:1212–1226.
22. Zhao Q, Manohar M, Wei Y, et al. Sting signalling protects against chronic pancreatitis by modulating T<sub>H</sub>17 response. *Gut.* 2019;68:1827–1837.
23. Liu J, Xie X, Xuan C, et al. High-density infiltration of V-domain immunoglobulin suppressor of T-cell activation up-regulated immune cells in human pancreatic cancer. *Pancreas.* 2018;47:725–731.
24. Zhou Q, Xia S, Guo F, et al. Transforming growth factor-B in pancreatic diseases: mechanisms and therapeutic potential. *Pharmacol Res.* 2019;142:58–69.
25. Tu J, Guo Y, Hong W, et al. The regulatory effects of paeoniflorin and its derivative paeoniflorin-6'-O-benzene sulfonate CP-25 on inflammation and immune diseases. *Front Pharmacol.* 2019;10:57.
26. Tian R, Wang RL, Xie H, et al. Overexpressed miRNA-155 dysregulates intestinal epithelial apical junctional complex in severe acute pancreatitis. *World J Gastroenterol.* 2013;19:8282–8291.
27. Förster C. Tight junctions and the modulation of barrier function in disease. *Histochem Cell Biol.* 2008;130:55–70.
28. Lei Q, Qiang F, Chao D, et al. Amelioration of hypoxia and LPS-induced intestinal epithelial barrier dysfunction by emodin through the suppression of the NF- $\kappa$ B and HIF-1 $\alpha$  signaling pathways. *Int J Mol Med.* 2014;34:1629–1639.
29. Xia XM, Li BK, Xing SM, et al. Emodin promoted pancreatic claudin-5 and occludin expression in experimental acute pancreatitis rats. *World J Gastroenterol.* 2012;18:2132–2139.
30. Liu MW, Wei R, Su MX, et al. Effects of Panax notoginseng saponins on severe acute pancreatitis through the regulation of mTOR/Akt and caspase-3 signaling pathway by upregulating miR-181b expression in rats. *BMC Complement Altern Med.* 2018;18:51.
31. Wen Y, Liu R, Lin N, et al. NADPH oxidase hyperactivity contributes to cardiac dysfunction and apoptosis in rats with severe experimental pancreatitis through ROS-mediated MAPK signaling pathway. *Oxid Med Cell Longev.* 2019;2019:4578175.
32. Nuñez G, Benedict MA, Hu Y, et al. Caspases: the proteases of the apoptotic pathway. *Oncogene.* 1998;17:3237–3245.
33. Sendlir M, van den Brandt C, Glaubit J, et al. NLRP3 inflammasome regulates development of systemic inflammatory response and compensatory anti-inflammatory response syndromes in mice with acute pancreatitis. *Gastroenterology.* 2020;158:253–269.e14.
34. Jochheim LS, Odysseos G, Hidalgo-Sastre A, et al. The neuropeptide receptor subunit RAMP1 constrains the innate immune response during acute pancreatitis in mice. *Pancreatol.* 2019;19:541–547.
35. Gunjaca I, Zunic J, Gunjaca M, et al. Circulating cytokine levels in acute pancreatitis-model of SIRS/CARS can help in the clinical assessment of disease severity. *Inflammation.* 2012;35:758–763.
36. Minkov GA, Yovtchev YP, Halacheva KS. Increased circulating CD4+CD25+CD127low/Neg regulatory T-cells as a prognostic biomarker in acute pancreatitis. *Pancreas.* 2017;46:1003–1010.
37. Xiong Y, Chen L, Fan L, et al. Free total rhubarb anthraquinones protect intestinal injury via regulation of the intestinal immune response in a rat model of severe acute pancreatitis. *Front Pharmacol.* 2018;9:75.
38. Jensen KD, Su X, Shin S, et al. Thymic selection determines gammadelta T cell effector fate: antigen-naïve cells make interleukin-17 and antigen-experienced cells make interferon gamma. *Immunity.* 2008;29:90–100.
39. Turchinovich G, Pennington DJ. T cell receptor signalling in  $\gamma\delta$  cell development: strength isn't everything. *Trends Immunol.* 2011;32:567–573.
40. Muro R, Nitta T, Nakano K, et al.  $\gamma\delta$ TCR recruits the Syk/PI3K axis to drive proinflammatory differentiation program. *J Clin Invest.* 2018;128:415–426.
41. Shibata K. Close link between development and function of gamma-delta T cells. *Microbiol Immunol.* 2012;56:217–227.
42. Sasikala M, Ravikanth VV, Murali Manohar K, et al. Bach2 repression mediates T<sub>H</sub>17 cell induced inflammation and associates with clinical features of advanced disease in chronic pancreatitis. *United European Gastroenterol J.* 2018;6:272–282.
43. Akitsu A, Iwakura Y. Interleukin-17-producing  $\gamma\delta$  T ( $\gamma\delta$ 17) cells in inflammatory diseases. *Immunology.* 2018;155:418–426.
44. Yan K, Yang J, Qian Q, et al. Pathogenic role of an IL-23/ $\gamma\delta$ T17/neutrophil axis in coxsackievirus B3-induced pancreatitis. *J Immunol.* 2019;203:3301–3312.
45. Zhou R, Zhang J, Bu W, et al. A new role for the spleen: aggravation of the systemic inflammatory response in rats with severe acute pancreatitis. *Am J Pathol.* 2019;189:2233–2245.